DOI: 10.1002/chem.200903214

Microwave Irradiation for the Facile Synthesis of Transition-Metal Nanoparticles (NPs) in Ionic Liquids (ILs) from Metal–Carbonyl Precursors and Ru-, Rh-, and Ir-NP/IL Dispersions as Biphasic Liquid–Liquid Hydrogenation Nanocatalysts for Cyclohexene

Christian Vollmer,[a] Engelbert Redel,[a] Khalid Abu-Shandi,[a, b] Ralf Thomann,[c] Haresh Manyar,[d] Christopher Hardacre,[d] and Christoph Janiak*[a]

Abstract: Stable chromium, molybdenum, tungsten, manganese, rhenium, ruthenium, osmium, cobalt, rhodium, and iridium metal nanoparticles (M-NPs) have been reproducibly obtained by facile, rapid (3 min), and energy-saving 10 W microwave irradiation (MWI) under an argon atmosphere from their metal–carbonyl precursors $[M_x(CO)_y]$ in the ionic liquid (IL) 1-butyl-3-methylimidazolium tetrafluoroborate ([BMIm][BF_4]). This MWI synthesis is compared to UV-photolytic (1000 W, 15 min) or conventional thermal decomposition (180–250 °C, 6–12 h) of $[M_x(CO)_y]$ in ILs. The MWI-obtained nanoparticles have a very small (< 5 nm) and uniform size and are prepared without any additional stabilizers or capping molecules as long-term stable M-NP/IL dispersions (characterization by transmission electron microscopy (TEM), transmission electron diffraction (TED), and dynamic light scattering (DLS)). The ruthenium, rhodium, or iridium nanoparticle/IL dispersions are highly active and easily recyclable catalysts for the biphasic liquid–liquid hydrogenation of cyclohexene to cyclohexane with activities of up to 522 (mol product) (mol Ru)$^{-1}$ h^{-1} and 884 (mol product) (mol Rh)$^{-1}$ h^{-1} and give almost quantitative conversion within 2 h at 10 bar H_2 and 90 °C. Catalyst poisoning experiments with CS_2 (0.05 equiv per Ru) suggest a heterogeneous surface catalysis of Ru-NPs.

Keywords: heterogeneous catalysis · hydrogenation · ionic liquids · nanoparticles · transition metals

Introduction

Metal nanoparticles (M-NPs) are of significant interest for technological applications in several areas of science and industry, especially in catalysis due to their high activity. In particular, Rh- and Ru-NPs can be used for olefin hydrogenation.[1] The controlled and reproducible synthesis of defined and stable M-NPs is very important for a range of applications.[2–7] M-NPs can be synthesized in ionic liquids (ILs)[8] through chemical reduction[9–13] or decomposition[14] of metal salts or metal complexes, and by means of photochemical[15,16] or electroreduction,[17–19] without the need of extra stabilizing molecules or organic solvents.[20–22] Recently, we communicated the preparation of transition-metal nanoparticles by thermal decomposition of metal carbonyls in ILs.[23–26]

Here we investigate the use of microwave irradiation for the synthesis of M-NPs. Microwave heating is extremely rapid. Microwaves are a low-frequency energy source that is remarkably adaptable to many types of chemical reac-

[a] C. Vollmer, Dr. E. Redel, Prof. Dr. K. Abu-Shandi, Prof. Dr. C. Janiak
Institut für Anorganische und Analytische Chemie
Universität Freiburg
Albertstrasse 21, 79104 Freiburg (Germany)
E-mail: janiak@uni-freiburg.de

[b] Prof. Dr. K. Abu-Shandi
Permanent address:
Department of Chemistry, Tafila Technical University
P.O. Box 179, Tafila 66110 (Jordan)

[c] Dr. R. Thomann
FMF (Freiburger Material Forschungszentrum), Universität Freiburg
Stefan-Meier-Strasse 21, 79104 Freiburg (Germany)

[d] Dr. H. Manyar, Prof. Dr. C. Hardacre
CenTACat, School of Chemistry and Chemical Engineering
Queen's University Belfast
Stranmillis Road, Belfast, BT9 5AG, Northern Ireland (UK)

Supporting information for this article is available on the WWW under http://dx.doi.org/10.1002/chem.200903214. It contains materials and instrumentation, experimental details, pictures of M-NP/IL dispersions, Raman-FT spectra, additional TEM and TED pictures, and statistical graphs for DLS.

tions.[27] Microwave radiation can interact directly with the reaction components: the reactant mixture absorbs the microwave energy and localized superheating occurs resulting in fast and efficient heating.[28] Using microwaves is a fast way to heat reactants compared with conventional thermal heating. Any presumptions about abnormal "microwave effects"[29–31] have been proven wrong in the literature.[32,33] Moreover, microwave reactions are also an "instant on/instant off" energy source, significantly reducing the risk of overheating reactions.[27,28] Furthermore, ILs seems to be an ideal media for microwave reactions and have significant absorption efficiency for microwave energy because of their high ionic charge, high polarity, and high dielectric constant.[34]

ILs act as a "novel nanosynthetic template"[23] that stabilizes M-NPs on the basis of the ionic charge, high polarity, high dielectric constant, and supramolecular network of the IL.[35] According to DLVO (Derjaguin–Landau–Verwey–Overbeek) theory,[36] ILs provide an electrostatic protection in the form of a "protective shell" for M-NPs.[20,26,37–39] DLVO theory predicts that the first inner shell must be anionic and that the anion charges should be the primary source of stabilization for the electrophilic metal nanocluster.[36] Experimentally PF_6^- anions were found on a Pd nanocluster surface prepared in [BMIm][PF_6] by X-ray photoelectron spectroscopy.[40] DLVO theory treats anions as ideal point charges. Real-life anions with a molecular volume would be classified as "electrosteric stabilizers". However, the term "electrosteric" is contentious and ill-defined.[41] The stabilization of metal nanoclusters in ILs could, thus, be attributed to "extra-DLVO" forces,[41] which includes effects from the network properties of ILs such as hydrogen bonding, the hydrophobicity, and steric interactions.[3,42] When mixed with other molecules or M-NPs, ILs become nanostructured materials with polar and nonpolar regions.[43–46] For M-NP synthesis in ILs, a correlation was found between the molecular volume of the IL anion and the size of the synthesized M-NPs.[9,24,25] In M-NPs synthesized through sol–gel, microemulsion, and other processes with stabilizers or capping molecules, the concentration of the precursor plays a crucial role in determining the particle size and size distribution.[20]

In the absence of strongly coordinating protective ligand layers, M-NPs in ILs should be effective catalysts. The IL network contains only weakly coordinating cations and anions that bind less strongly to the metal surface and, hence, are less deactivating than the commonly employed capping ligands. The combination of M-NPs and ILs can be considered a *green catalytic system*. ILs are interesting in the context of green catalysis,[47] which requires that catalysts be designed for easy product separation from the reaction products and with efficient and multiple reuse/recycling.[34,48] Firstly, the very low vapor pressure of the IL and designable low miscibility of ILs with organic solutes allows for a facile separation of volatile products by distillation or removal in vacuum. Secondly, the IL is able to retain the M-NPs for catalyst reuse. For example, Dupont and co-workers have shown that a M-NP/IL system can be recycled quite easily and can be reused several times without any significant changes in catalytic activity.[12] As we recently reported for Rh-NP/IL in a hydrogenation reaction, the catalytic activity can, in some cases, even increase upon reuse.[24] A sizable number of catalytic reactions have successfully been carried out in ILs.[49] Generally, the catalytic properties (activity and selectivity) of dispersed M-NPs indicate that they possess pronounced surfacelike (multisite) rather than single-site-like character.[50]

The hydrogenation of benzene to cyclohexane is a multimillion-ton process due to the subsequent oxidation of the cyclohexane to adipic acid and caprolactam, which are building blocks for Nylon 6.6 and Nylon 6.[51,52] Cyclohexene is often taken as a model substrate for hydrogenation activity studies of biphasic liquid–liquid systems involving ILs[53–55] because its solubility is limited in [BMIm][BF_4].[56]

Herein we report the facile, rapid (3 min), and energy-saving preparations of transition M-NPs from their carbonyl precursors by microwave irradiation in the IL [BMIm][BF_4]. Through this metal–carbonyl decomposition we very quickly generate M-NP/IL dispersions that are catalytically highly active in the repeated catalytic model hydrogenation of cyclohexene with M = Ru, Rh, and Ir.

Abstract in German: *Stabile Chrom-, Molybdän-, Wolfram-, Mangan-, Rhenium-, Ruthenium-, Osmium-, Cobalt-, Rhodium- und Iridium-Metall-Nanopartikel (M-NP) werden reproduzierbar durch einfache, schnelle (3 min) und energiesparende 10 W Mikrowellenbestrahlung (MWI) unter Argonatmosphäre aus ihren Metallcarbonyl-Ausgangsverbindungen [$M_x(CO)_y$] in der ionischen Flüssigkeit (IL) 1-Butyl-3-methylimidazolium-tetrafluoroborat ([BMIm][BF_4]) erhalten. Diese MWI-Synthese wird mit der UV-photolytischen (1000 W, 15 min) oder konventionellen thermischen Zersetzung (180–250 °C, 6–12 h) von [$M_x(CO)_y$] in ILs verglichen. Die mit MWI erhaltenen Nanopartikel haben eine sehr kleine (< 5 nm) und einheitliche Größe und werden ohne zusätzliche Stabilisatoren oder Oberflächen-bedeckende Liganden als langzeitstabile M-NP/IL-Dispersionen erhalten (Charakterisierung durch Transmissionselektronenmikroskopie (TEM), Transmissionselektronenbeugung (TED) und dynamische Lichtstreuung (DLS)). Die Ruthenium-, Rhodium- oder Iridium-Nanopartikel/IL-Dispersionen sind hoch aktive und leicht wieder zu verwendende Katalysatoren für die Zweiphasen-flüssig-flüssig-Hydrierung von Cyclohexen zu Cyclohexan, mit Aktivitäten bis zu 522 (mol Produkt) (mol Ru)$^{-1}$ h^{-1} und 884 (mol Produkt) (mol Rh)$^{-1}$ h^{-1} und beinahe quantitativem Umsatz innerhalb 2 h bei 10 bar H_2 und 90 °C. Katalysatorvergiftungsexperimente mit CS_2 (0.05 Äquivalent pro Ru) sprechen für eine heterogene Oberflächenkatalyse von Ru-NPs.*

Results and Discussion

M-NP synthesis and characterization: The metal carbonyl $[Cr(CO)_6]$, $[Mo(CO)_6]$, $[W(CO)_6]$, $[Mn_2(CO)_{10}]$, $[Re_2(CO)_{10}]$, $[Fe_2(CO)_9]$, $[Ru_3(CO)_{12}]$, $[Os_3(CO)_{12}]$, $[Co_2(CO)_8]$, $[Rh_6(CO)_{16}]$, or $[Ir_6(CO)_{16}]$ was dissolved/suspended under an argon atmosphere in dried and deoxygenated $[BMIm][BF_4]$. Decomposition by microwave irradiation of the metal carbonyl in the IL was achieved after only 3 min using a low power of 10 W (Scheme 1) under argon.

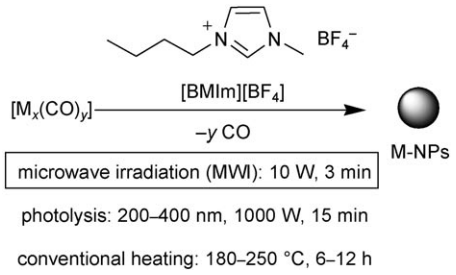

Scheme 1. Microwave, photolytic, and thermal decomposition of metal carbonyls to M-NPs.

We used a low energy of 10 W on a vial of 10 mL filled with 0.48 g IL. Within less than 1 min of microwave radiation a temperature of 250 °C was reached. For the photolytic decomposition (only partly reported previously),[9,23,24] the mixture was irradiated under an argon atmosphere using a 1000 W UV-light source between 200 and 450 nm for 15 min. This has to be compared to the previously reported thermal M-NP synthesis in which the mixture had to be heated up to 250 °C for several hours under argon to decompose the metal carbonyl.[9,23,24]

The obtained dispersions had different colors: green Cr-, orange-red Os-, and yellow Mn- and W-NP dispersions; and dark-brown to black Mo-, Re-, Ru-, Co-, Rh-, or Ir-NP dispersions (Figure S2 in the Supporting Information) were reproducibly obtained through microwave decomposition at 10 W in 3 min from their metal carbonyl in $[BMIm][BF_4]$. Complete $[M_x(CO)_y]$ decomposition from the short, 3 min microwave irradiation was verified by Raman spectroscopy with no (metal–)carbonyl bands between 1750 and 2000 cm^{-1} being observed any more after the microwave treatment (Figure 1; and Figures S3–S6 in the Supporting Information).

The resulting M-NPs were analyzed by transmission electron microscopy (TEM; Figures 2–6), transmission electron diffraction (TED), and dynamic light scattering (DLS) for their size and size distribution (Table 1). The hydrodynamic radius from DLS is roughly two to three times the size of the pure kernel cluster. For very small M-NPs ($\approx$1 nm) the size of the hydrodynamic radius was found to be more than three times the radius found from TEM.

The median M-NP diameter for the microwave-synthesized Cr-, Mo-, W-, Re-, Ru-, Os-, Rh-, and Ir-NPs was between 0.7 and 3.1 nm, which is extremely small, and had a narrow and uniform, albeit not monodisperse, size distribution (TEM data in Table 1). It is, at present, not trivial to routinely and easily prepare uniform nanoparticles in the size range between 0.8–2.4 nm. No extra stabilizers or capping molecules are needed to achieve this small particle size (see below).

The median diameter of M-NPs from photolysis was between <1 to 4.4 nm with magnetic Co-NPs being larger (8.1 nm) (TEM data in Table 1).

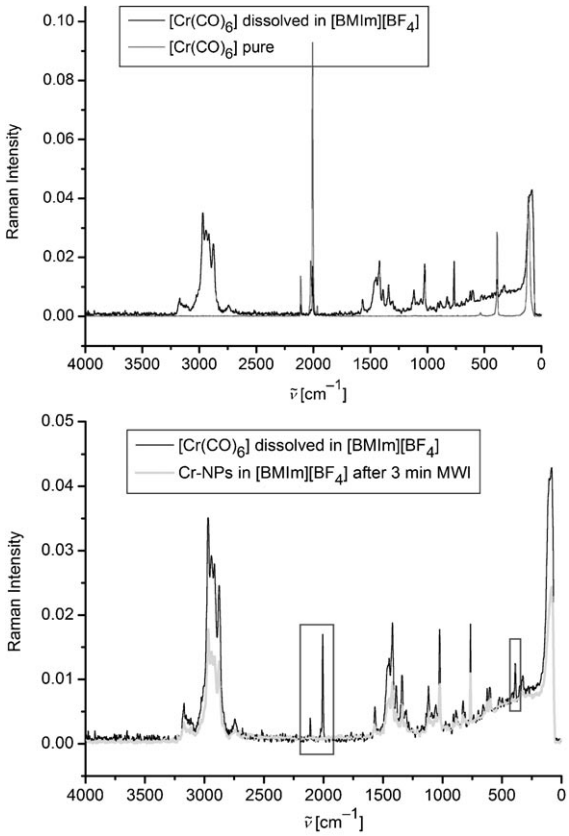

Figure 1. Raman-FT spectra. Top: pure metal carbonyl and it dissolved in $[BMIm][BF_4]$; bottom: before and after microwave irradiation (MWI; 3 min, 10 W) with the samples dissolved in $[BMIm][BF_4]$. The boxes highlight the indicative metal–carbonyl carbonyl bands (for further Raman-FT spectra see Figures S3–S6 in the Supporting Information).

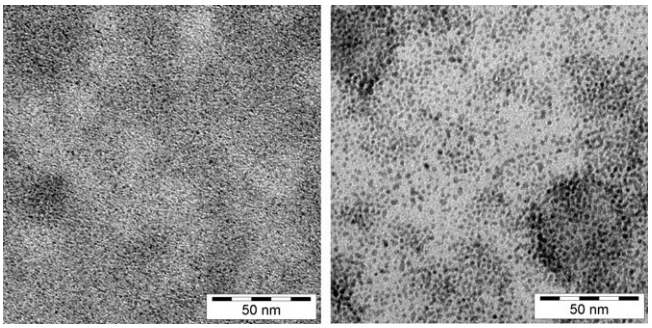

Figure 2. Rh-NPs from $[Rh_6(CO)_{16}]$ by MWI (left) and thermal decomposition (right) (entry 10a in Table 1).

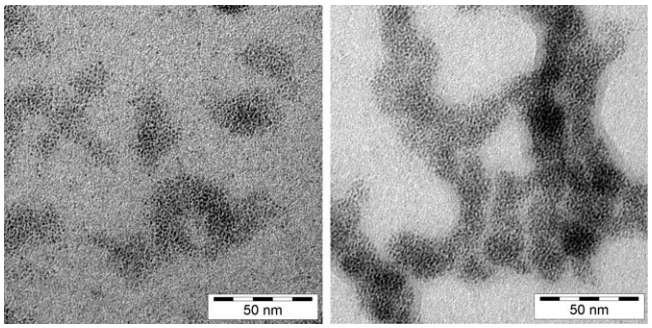

Figure 3. Ir-NPs from $[Ir_6(CO)_{16}]$ by MWI (left) and photolytic decomposition (right) (entry 11 in Table 1). TEM pictures with particles of median diameter of less than 1.5 nm show electron-dense cloudy structures due to scattering by the surrounding IL so that resolution of the TEM is limited and particles below 1.5 nm are hardly resolved.[25]

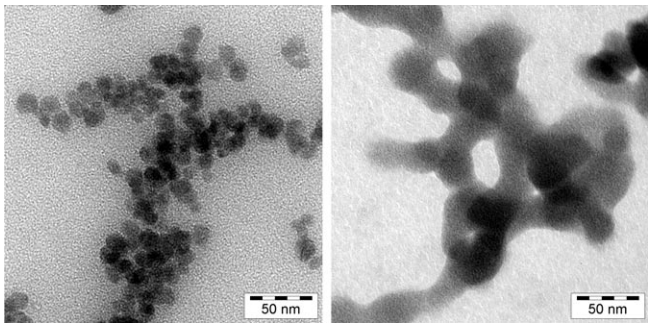

Figure 4. Mn-NPs from $[Mn_2(CO)_{10}]$ by MWI (left) and photolytic decomposition (right) ($Ø < 1$ nm, see comment in Figure 3; entry 4 in Table 1).

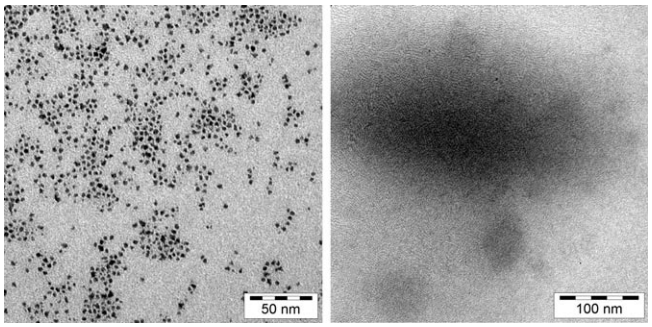

Figure 5. Re-NPs from $[Re_2(CO)_{10}]$ by MWI (left) and photolytic decomposition (right) ($Ø < 1$ nm, see comment in Figure 3; entry 5 in Table 1).

The conventional thermal heating decomposition of metal carbonyls to M-NPs yielded median diameters mostly between 1.1 and 3.5 nm. For the magnetic Fe-NPs and Co-NPs the median diameter was somewhat larger with 5.2 and 14 nm, respectively (TEM data, Table 1).

In comparison, the Os-, (magnetic) Co-, Rh-, and Ir-NPs from microwave synthesis are smaller than those obtained by photolysis and conventional heating. Nonmagnetic Mn-NPs present an exception as their microwave-derived particle size is considerably larger (12.4 nm) than the photolytic-derived median diameter of approximately 1.0 nm (TEM data, Table 1).

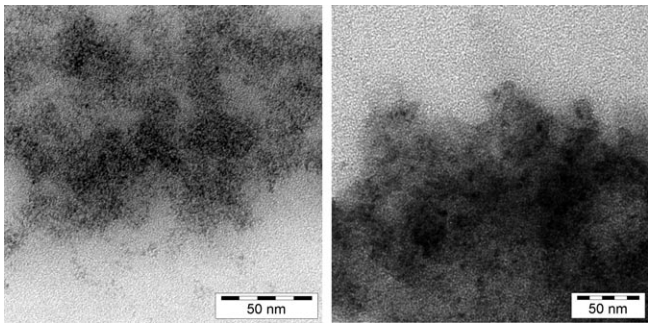

Figure 6. Mo-NPs from $[Mo(CO)_6]$ by MWI (left) and photolytic decomposition (right) ($Ø = 1$–2 nm, see comment in Figure 3; entry 2 in Table 1).

TEM photographs in Figures 2–6 illustrate that MWI (left pictures) tends to give better separated, that is, less-clustered M-NPs than photolytic decomposition (right pictures). Presumably this is due to the shorter reaction and heating time (3 min only).

The effect of varying the microwave irradiation time was examined for the decomposition of $[Ru_3(CO)_{12}]$ and $[Rh_6(CO)_{16}]$ by using 3 and 10 min (entries 7a, 7b and 10a, 10b in Table 1). No significant change in particle size and distribution was evident. The dispersions are stable for more than six months under an argon atmosphere. Under air the black, magnetic Fe (from conventional heating) and Co dispersions change their color and lose their magnetic properties.[23] The Ru, Rh, and Ir dispersions are stable, and their particle size did not change even after more than 70 h under an atmosphere of air/oxygen.[23,24] TED studies show that the Ru and Rh diffraction patterns correspond to their metal lattices (Figures 7 and 8; Tables S6 and S7 in the Supporting Information)[57] thereby proving their metal character and the absence of significant oxidation.

Cyclohexene hydrogenation by M-NP/IL dispersions: The Ru-, Rh-, and Ir-NP dispersions, which were obtained by microwave decomposition of their metal carbonyls in [BMIm]-$[BF_4]$ (Table 1), were tested for their catalytic activity in the biphasic liquid–liquid hydrogenation of cyclohexene to cyclohexane (Scheme 2). The low miscibility of substrates and products with the IL phase allows for easy separation by simple decantation of the hydrophobic phase. Cyclohexene was chosen as a substrate since it presents a challenge because of its low solubility in $[BMIm][BF_4]$ and is an intermediate in the hydrogenation of benzene to cyclohexane.[51,52]

In the context of green catalysis, the recyclability of the Ru-NPs/IL system was investigated. The hydrogenation reaction was run with a Ru-NP/$[BMIm][BF_4]$ dispersion and cyclohexene at 90 °C and 10 bar H_2 to 95 % conversion (Figure 9, entries 1–7 in Table 2; see also Table S4 in the Supporting information). The reaction was intentionally stopped at 95 % conversion as thereafter the decrease in cy-

Table 1. M-NP (M = Cr, Mo, W, Re, Mn, Fe, Ru, Os, Co, Rh, and Ir) size and size distribution[a] in [BMIm][BF_4] obtained by using different methods.

Entry	Metal carbonyl	Microwave decomposition[b]		Photolytic decomposition[c]		Thermal decomposition[d]	
		TEM Ø (σ) [nm]	DLS Ø[e] (σ) [nm]	TEM Ø (σ) [nm]	DLS Ø[e] (σ) [nm]	TEM Ø (σ) [nm]	DLS Ø[e] (σ) [nm]
1	$[Cr(CO)_6]$	$\leq$1.5 ($\pm$0.3)[f]	3.8 ($\pm$0.8)	4.4 ($\pm$1.0)	7.1 ($\pm$0.3)	$\leq$1.5 ($\pm$0.3)[g]	3.0 ($\pm$0.6)[g]
2	$[Mo(CO)_6]$	$\approx$1–2	4.5 ($\pm$0.8)	$\approx$1–2[g]	3.8 ($\pm$1.1)[g]	$\leq$1.5 ($\pm$0.3)[g]	2.5 ($\pm$0.6)[g]
3	$[W(CO)_6]$	3.1 ($\pm$0.8)	5.2 ($\pm$1.2)	$<$1	10.8 ($\pm$0.5)	$\leq$1.5 ($\pm$0.3)[g]	3.1 ($\pm$0.5)[g]
4	$[Mn_2(CO)_{10}]$	12.4 ($\pm$3)[h]	29 ($\pm$5.0)[h]	$<$1	2.5 ($\pm$0.8)	–	–
5	$[Re_2(CO)_{10}]$	2.4 ($\pm$0.9)	5.7 ($\pm$1.4)	$<$1	7.2 ($\pm$2.2)	–	–
6	$[Fe_2(CO)_9]$	8.6 ($\pm$3.2)[i]	12.8 ($\pm$0.6)[i]	7.0 ($\pm$3.1)[i]	12.5 ($\pm$0.5)[i]	5.2 ($\pm$1.6)[g]	10.1 ($\pm$2.1)[g]
7a	$[Ru_3(CO)_{12}]$	1.6 ($\pm$0.3)	a) 3.2 ($\pm$0.8)	2.0 ($\pm$0.5)[g]	3.9 ($\pm$1.0)[g]	1.6 ($\pm$0.4)[g]	2.9 ($\pm$0.5)[g]
7b		1.6 ($\pm$0.3)[j]	b) 3.2 ($\pm$0.8)[j]				
8	$[Os_3(CO)_{12}]$	0.7 ($\pm$0.2)	2.8 ($\pm$0.7)	2.0 ($\pm$1.0)	2.1 ($\pm$0.4)	2.5 ($\pm$0.4)[g,k]	5.6 ($\pm$1.5)[l]
9	$[Co_2(CO)_8]$	5.1 ($\pm$0.9)	20 ($\pm$3)	8.1 ($\pm$2.5)	12.6 ($\pm$0.4)	14 ($\pm$8)[g]	–
10a	$[Rh_6(CO)_{16}]$	1.7 ($\pm$0.3)	3.7 ($\pm$0.6)	1.9 ($\pm$0.3)	5.5 ($\pm$0.4)	3.5 ($\pm$0.8)[g]	7.0 ($\pm$1.2)[g]
10b		1.7 ($\pm$0.3)[j]	3.4 ($\pm$0.5)[j]				
11	$[Ir_6(CO)_{16}]$	0.8 ($\pm$0.2)	3.3 ($\pm$0.9)	1.4 ($\pm$0.3)	4.1 ($\pm$1.2)	1.1 ($\pm$0.2)[g]	4.1 ($\pm$0.7)[g]

[a] Median diameters (Ø) and standard deviations (σ) are for a single TEM or DLS experiment. Reproducibility of the particle size and distribution was insured by selected repeated TEM experiments and especially by DLS, which was carried out for almost all repeated decomposition reactions. [b] Microwave decomposition of metal carbonyls with 10 W for 3 min unless mentioned otherwise. [c] Photolytic decomposition of metal carbonyls with a 1000 W Hg lamp (200–450 nm wavelength) for 15 min. [d] Thermal decomposition of metal carbonyls from 6–12 h with 180–230 °C depending on the metal carbonyl. [e] Hydrodynamic radius, median diameter from the first 3 measurements at 633 nm. The hydrodynamic radius is roughly 2–3 times the size of the pure kernel cluster. For very small M-NPs ($\approx$1 nm) the size of the hydrodynamic radius can even increase to more than 3 times the M-NP radius. The resolution of the DLS instrument is 0.6 nm. Solubility of metal–carbonyl precursors in [BMIm][BF_4] is limited to a maximum value of about 1 wt % of M. Statistical evaluation of the total sample pictures (see the Supporting Information). [f] TEM pictures with particles of median diameter of less than 1.5 nm show electron-dense cloudy structures due to scattering by the surrounding IL so that resolution of the TEM is limited and particles below 1.5 nm are hardly resolved. [g] Data from refs. [23–25]. [h] $[Mn_2(CO)_{10}]$ was of a larger grain size than all the other metal carbonyls that came as fine powders. Also, upon grinding in a mortar, $[Mn_2(CO)_{10}]$ could not be ground as finely as the other metal carbonyls. [i] TEM/TED analyses of the nanoparticles from the microwave and photolytic decomposition of $[Fe_2(CO)_9]$ show the presence of Fe_2O_3. Because of the experimental setup, rigorous air exclusion is more difficult during microwave irradiation and photolysis and workup. [j] Microwave decomposition of metal carbonyls with 10 W for 10 min. [k] 0.2 wt % $[Os_3(CO)_{12}]$ in [BMIm][BF_4]. [l] 1 wt % $[Os_3(CO)_{12}]$ in [BMIm][BF_4].

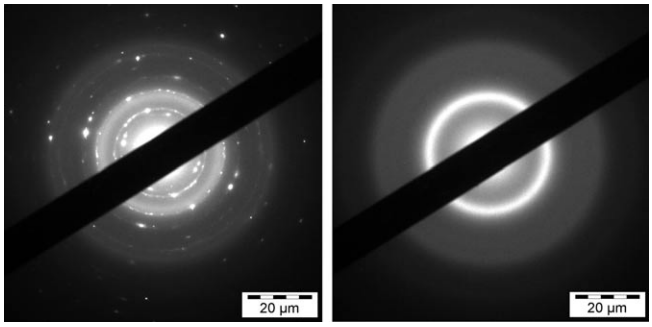

Figure 7. TED pattern of Ru nanoparticles from $[Ru_3(CO)_{12}]$ in [BMIm]-[BF_4] by microwave (left) and thermal decomposition (right) (entries 7a and 7b, respectively, in Table 1). The black bar is the beam stopper. The diffraction rings at 2.1 Å (very strong); 1.6, 1.4, and 1.1 Å (all weak) match with the *d* spacing of the Ru diffraction pattern (see Table S6 in the Supporting Information).

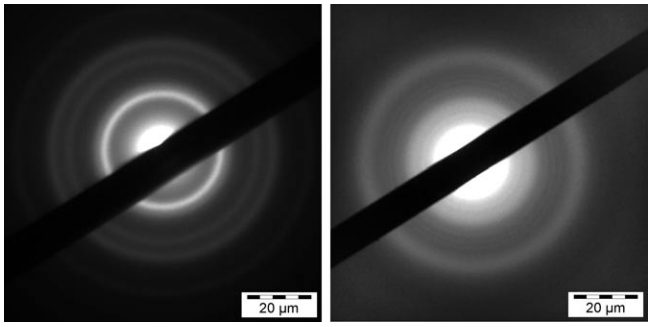

Figure 8. TED pattern of Rh-NPs from $[Rh_6(CO)_{16}]$ in [BMIm][BF_4] by microwave (left) and thermal decomposition (right) (entries 10a and 10b, respectively, in Table 1). The black bar is the beam stopper. The diffraction rings at 2.2 Å (very strong); 1.9, 1.4, and 1.1 Å (all strong) match with the *d* spacing of the Rh diffraction pattern (see Table S7 in the Supporting Information).

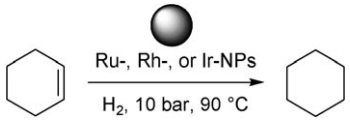

Scheme 2. Hydrogenation of cyclohexene to cyclohexane with Ru-, Rh-, or Ir-NPs.

clohexene concentration lowered the reaction rate (Figure 9). At 95 % conversion, adjudged by the H_2 consumption, the reactor was depressurized, the organic layer was decanted, and fresh cyclohexene (20 mL) was added. The Ru dispersions were then reused at least six times with an increase of the catalytic activity from 293 for the first to 522 (mol product)(mol metal)$^{-1}$ h^{-1} for the seventh run (entries 1–7 in Table 2, Figure 10). In the first run 216 min were needed to achieve 95 % conversion, whereas in the seventh run, 95 % conversion was obtained after 120 min (Figures 9 and 11, Table 2). This is contrary to previous reports that describe a decrease of the catalytic activity for the hydrogenation of arenes.[11]

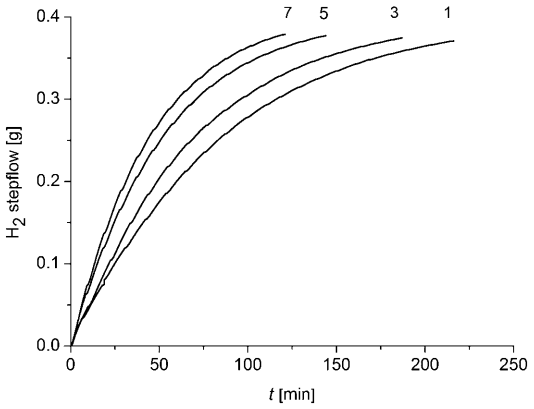

Figure 9. H_2 uptake over time for the 1st, 3rd, 5th, and 7th hydrogenation run of cyclohexene (20 mL, 0.2 mol) to cyclohexane with the same 1 wt% Ru-NP/[BMIm][BF_4] catalyst (0.18 mmol Ru in 1.5 mL IL) and molar cyclohexene/metal ratio of 1108 at 90°C, 10 bar H_2 pressure (cf. Table 2). An H_2 uptake of 0.38 g corresponds to 95% conversion (100% are 0.2 mol or 0.4 g H_2). H_2 uptake for the additional 2nd, 4th, and 6th run are included in Figure S1 of the Supporting Information.

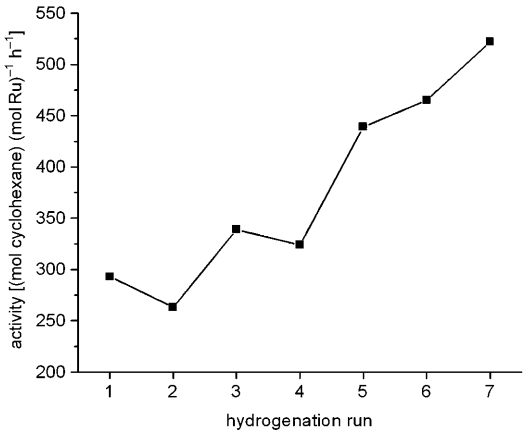

Figure 10. Activity for seven runs of the hydrogenation of cyclohexene (20 mL, 0.2 mol) with the same 1 wt% Ru-NP/[BMIm][BF_4] catalyst (0.18 mmol, 18 mg Ru in 1.5 mL, 1.8 g IL) and molar cyclohexene/metal ratio of 1108 at 90°C, 10 bar H_2 pressure, run to 95% conversion.

Table 2. Hydrogenation of cyclohexene to cyclohexane by M-NPs.[a]

	Catalyst[b]	t [min]	H_2 [bar]	T [°C]	Conversion [%]	Activity [(mol product) (mol metal)$^{-1}$ h^{-1}]
1	Ru/IL[b]	216	10	90	95	293
2	2nd run	240	10	90	95	263
3	3rd run	186	10	90	95	339
4	4th run	195	10	90	95	324
5	5th run	144	10	90	95	439
6	6th run	136	10	90	95	465
7	7th run	120	10	90	95	522
8	Ru/IL	220	4	75	42	129
9	Ru/silica[c]	70	4	75	5.0	–
10	Rh/IL[d]	88	10	90	90	695
11	2nd run	73	10	90	95	884
12	3rd run	78	10	90	95	810
13	Ir/IL	205	10	90	36	222
14	Ru/IL/CS_2[e]	120	10	25	0	0
15	Ru/IL/CS_2[e]	120	10	90	0	0

[a] Ratios: cyclohexene/Ru = 1108; cyclohexene/Rh = 1108; cyclohexene/Ir = 2108. [b] IL = [BMIm][BF_4]. 1 wt% Ru in IL: 0.18 mmol (18 mg) Ru in 1.5 mL (1.8 g) IL, prepared by microwave decomposition; 1 wt% Rh in IL: 0.18 mmol (18 mg) Rh in 1.5 mL (1.8 g) IL, prepared by microwave decomposition, 1 wt% Ir in IL: 0.09 mmol (18 mg) in 1.5 mL (1.8 g) IL, prepared by microwave decomposition. [c] Ruthenium on silica:[66] 100 mg of a 1 wt% Ru/silica powder, in cyclohexene (20 mL, 0.2 mol), no IL present. [d] The H_2 consumption for the 1st run was very low so that the 95% conversion would not have been reached within a reasonable time frame and the reaction was stopped after 88 min. [e] CS_2 (0.009 mmol, 0.68 mg, 0.54 μL, density 1.266 g cm^{-3}, corresponding to 0.05 equiv (5 mol%) of Ru) was dissolved in cyclohexene (20 mL, 0.2 mol). The mixture was added to the Ru/IL dispersion before pressurizing the reactor and the possible hydrogenation was given 2 h at 90°C and 10 bar H_2 pressure. No conversion could be detected by GC analysis.

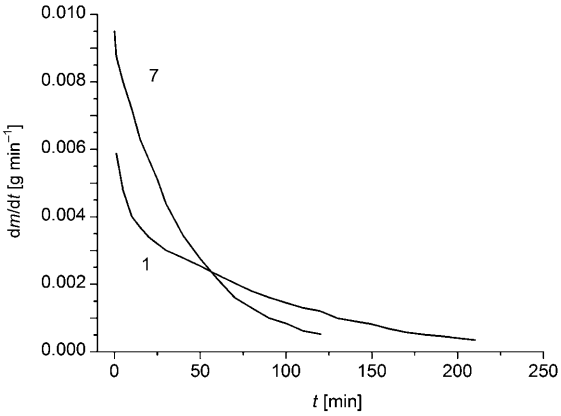

Figure 11. Reaction rate of the 1st and 7th run of cyclohexene to cyclohexane hydrogenation (cf. Figure 9, Figure 10, and Table 2).

The increase in initial reaction rate with recycling (Figures 9 and 11) cannot be due to the formation of Ru–hydride species. An induction period would be observed once if it was the case but not each time. The activity rise with each recycle may be due to surface restructuring and/or the formation of active Ru–N-heterocyclic carbene (NHC)[58] surface species. It is likely that the rate of restructuring or NHC–Ru formation reactions is slow and therefore the continuous formation of defects, edges, corners, or steps on the surface, which are known to be more-active sites,[59] will gradually increase the catalytic activity. In the case of Ir nanoclusters stabilized by imidazolium ILs, it was found that NHCs form at the surface of the nanocluster from the IL cation.[60] Based on work of Pd-NP/Pd-atom catalyzed C–C coupling reactions we may also envision a mechanism in which the Ru-NPs act as 'reservoirs' of active Ru clusters, atoms, or ions, which leach from the Ru-NPs to act as homogeneous catalysts.[61] The formation of this active catalyst form can be slow so that even after seven runs the production of active species is still progressing. The activity in-

crease is even more remarkable since the Ru-NP surface size may decrease over the runs through particle aggregation as suggested by TEM pictures of the used Ru-NP/[BMIm]-[BF_4] catalyst dispersion (Figure 12). TEM pictures were

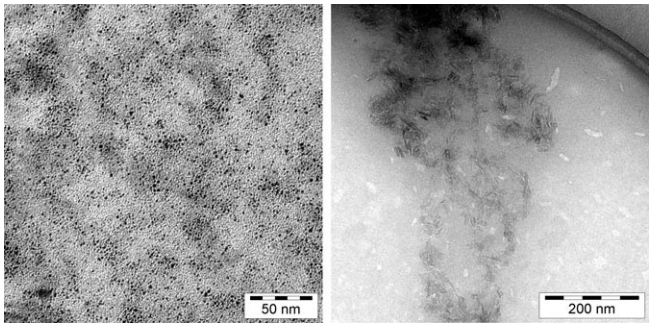

Figure 12. Ru-NPs synthesized in [BMIm][BF_4] under microwave conditions before being used in the catalytic hydrogenation (left) and after the 7th run (right).

taken from the Ru-NPs before the catalytic hydrogenation and after the seventh run (Figure 12). The unused Ru-NPs are spherical with a size of (1.6 ± 0.3) nm (cf. entry 7 in Table 1). After the seventh run the particles have transformed into rods with a length of (18 ± 7) nm and a width of (5 ± 2) nm.

We note that activity calculations with M-NPs are typically based on the total amount of metal and neither the surface of the exposed metal nor the possibly leached atoms. Different studies show that the catalytic activity results not just from the exposed surface metal atoms. During heterogeneous catalysis the surface can reconstruct and these changes make it difficult to determine the number of surface atoms. Partial aggregation is also possible during catalysis, which would have a strong influence on the fraction of the surface atoms present. Heterogeneous catalytic reactions are extremely complex and it is also possible that atoms under the exposed surface atoms play a significant role in the catalytic activity. Moreover, defects, the surface topology, and surface atom sides (edges, corners, steps) rather than the sole amount of surface atoms strongly influence the catalytic activity not to mention the possibility of atom leaching with a homogeneous activity.[59,61]

To differentiate between possible homogeneous Ru atom and heterogeneous Ru-NP catalysts we have added CS_2 as a known ruthenium catalyst poison following the elegant work by Finke et al.[62,63] CS_2 binds strongly to active metal sites and blocks access of the substrates. If it is possible to poison a catalyst completely with $\ll1$ equiv ($\ll100$ mol%) of the added ligand per Ru atom, this is strong evidence that it is a heterogeneous catalyst. The reasoning is that in a heterogeneous (colloidal) metal-particle catalyst only a fraction of the metal atoms are on the surface, hence much less than a one molar equivalent of ligand per metal atom will be sufficient to deactivate the catalyst.[63,64] A molecular, homogeneous catalyst needs ≥1.0 equiv of the ligand (per metal atom) for the poisoning. The metal–ligand binding depends on the temperature. At higher temperatures ligands like CS_2 can dissociate from the metal atoms[65] and catalysis can occur. For two attempted catalytic runs at 25 and 90 °C in the presence of CS_2 (0.05 equiv, 5 mol% of Ru) we found that CS_2 completely poisons the Ru-NP catalyst (entries 14 and 15, Table 2). Even at 90 °C the CS_2 is bound to the active sites and no cyclohexene hydrogenation could be detected by GC analysis. Thus, less than 5% of the metal atoms of the Ru-NP are active (surface) sites. Conversely, the activity is >20 times higher on a per-active-metal-atom basis. We therefore suggest that the activity increase upon recycling is due to surface reconstruction creating more and more active sites.

The hydrogen pressure directly influences the activity. When the cyclohexene hydrogenation with a 1 wt% Ru-NP/[BMIm][BF_4] catalyst dispersion was decreased from 10 bar to 4 bar H_2 pressure (entry 9 in Table 2), the activity decreased significantly even when the activities were normalized to the pressure. The general (H_2) gas-to-liquid ([BMIm][BF_4]) phase diffusion rate requires a threshold pressure, that is, it requires the kinetic diffusion rate to be overcome for a linear increase of the activity with pressure since mass transport is a known problem in ILs.[67] Still the conversion of cyclohexene with Ru/IL at 4 bar is much higher than with a conventional Ru/silica catalyst in cyclohexene only (compare entries 8 and 9 in Table 2).

The catalytic activities and conditions in cyclohexene hydrogenations of Ru-NPs prepared from other precursors are listed in Table 3. It is evident that the catalytic properties of Ru-NPs/ILs are strongly influenced by the nature of the IL anion with BF_4^--based ILs yielding higher activities than those in the PF_6^--based ILs.[50]

Table 3. Catalyst activities of Ru-NPs in the biphasic liquid–liquid cyclohexene hydrogenation with $BMIm^+$-containing ILs.

Precursor[a]/M-NPs	IL anion	H_2 [bar]	Conversion [%]	Activity [(mol product) (mol metal)$^{-1}$ h^{-1}]	Ref.
[Ru(cod)(cot)]/Ru	BF_4^-	4	>99	100	[56]
	PF_6^-	4	>99	62	[56]
RuO_2/Ru	BF_4^-	4	100	388	[54]
[$Pd(acac)_2$]/Pd	PF_6^-	1	100	147	[55]

[a] cod = 1,5-cyclooctadiene, cot = 1,5-cyclooctatriene, and acac = acetylacetonate.

After the seventh hydrogenation run, the cyclohexane/cyclohexene mixture was decanted from the Ru-NP/IL dispersion to check for leaching of ruthenium metal into the product phase. The product mixture was evaporated to dryness and the residue was dissolved in concentrated (65%) nitric acid (10 mL) and analyzed by ICP-AES (inductively coupled plasma atomic emission spectroscopy). An Ru mass of 8.5×10^{-3} mg (84×10^{-9} mol) was found, which corresponds to less than 0.05% of the 18 mg (0.18 mmol) of Ru contained in the starting IL dispersion. Note that this Ru leach-

ing would be expected to be zero if the product were removed by vacuum distillation from the IL phase due to the low volatility of the IL and the NPs.

We recently reported the hydrogenation of cyclohexene to cyclohexane with Rh- and Ir-NPs using 4 bar H_2 pressure at 75 °C in a 120 mL Büchi glass autoclave or in a 30 mL glass inlay within a steel autoclave, both equipped with a magnetic stirring bar.[24] When using Rh dispersions obtained by microwave decomposition of $[Rh_6(CO)_{16}]$ in $[BMIm][BF_4]$ (entry 10 in Table 1) in the biphasic liquid–liquid hydrogenation of cyclohexene to cyclohexane under the reaction conditions of 90 °C and 10 bar (Scheme 2) an activity up to 884 (mol product) (mol metal)$^{-1}$ h^{-1} was attainable with 95 % conversion (Figure 13). The Rh dispersions

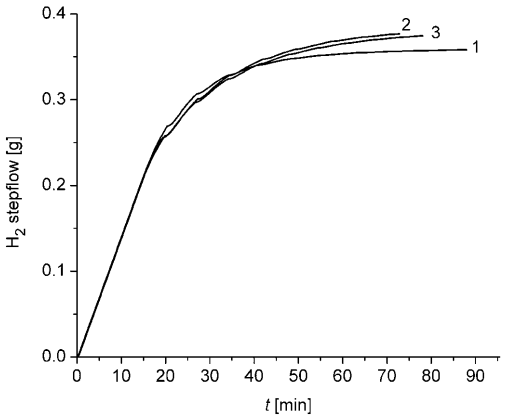

Figure 13. H_2 uptake over time for the three hydrogenation runs of cyclohexene (20 mL, 0.2 mol) to cyclohexane with the same 1 wt % Rh-NP/$[BMIm][BF_4]$ catalyst (0.18 mmol, 18 mg Rh in 1.5 mL, 1.8 g IL) and molar cyclohexene/metal ratio of 1128 at 90 °C, 10 bar H_2 pressure (cf. Table 2). An H_2 uptake of 0.38 g corresponds to 95 % conversion (100 % are 0.2 mol or 0.4 g H_2).

could be reused at least three times with an increase of the catalytic activity from 695 for the first to 884 (mol product) (mol metal)$^{-1}$ h^{-1} for the second run (entries 10–12 in Table 2 and Table S5 in the Supporting Information).

After the third hydrogenation run the cyclohexane/cyclohexene mixture was decanted from the Rh-NPs/IL dispersion to check for the leaching of rhodium into the product phase. The substrate/product mixture was evaporated to dryness and the residue was dissolved in concentrated (65 %) nitric acid (10 mL). An Rh mass of 0.01 mg (97×10^{-9} mol) was found, which corresponds to 0.05 % of the 18 mg (0.18 mmol) Rh contained in the starting IL dispersion.

The Ir-NP/IL dispersion, obtained by microwave decomposition of $[Ir_6(CO)_{16}]$ in $[BMIm][BF_4]$ (entry 11 in Table 1), was used in the biphasic liquid–liquid hydrogenation of cyclohexene to cyclohexane at 90 °C and 10 bar to yield an activity up to 222 (mol product) (mol metal)$^{-1}$ h^{-1}. Based on the condition shown in Scheme 2 the catalysis was started with the Ir-NPs/$[BMIm][BF_4]$ dispersion (1.5 mL, 1 wt %, 0.09 mmol) and cyclohexene (20 mL, 0.2 mol) (molar cyclohexene/metal ratio = 2108) at 90 °C and 10 bar H_2 to achieve 36 % conversion after 205 min.

Conclusion

We describe here a very simple, reproducible, and broadly applicable microwave, photolytic, or thermally induced metal–carbonyl decomposition for the synthesis of the most common transition-metal nanoparticles in the ionic liquid $[BMIm][BF_4]$. The M-NP sizes of about 0.8 to 5 nm for most of these transition-metal nanoparticles are extraordinary small and uniform with no extra stabilizers or capping molecules needed to achieve this small particle size in a long-term stable M-NP/IL dispersion. The synthesis uses easily available metal–carbonyl precursors and it is now shown that this method can readily be expanded to the broad range of all metal–carbonyl complexes. Microwave irradiation provides a very simple and reproducible way for the rapid (3 min) and energy-saving (10 W power) synthesis of defined and very small M-NPs from their binary metal–carbonyl complexes in ILs. The obtained Ru- and Rh-NP/IL dispersions can be used—without further treatment—as highly active and easily, multiply recyclable, heterogeneous hydrogenation catalysts, shown here for cyclohexene to cyclohexane conversion. Metal carbonyls are very attractive starting materials for nanosyntheses, commercially available in high purity or easily purified, for example, by sublimation. Furthermore, $[BMIm][BF_4]$ is now industrially available in large quantities.

Experimental Section

Materials and instrumentation for M-NP synthesis: $[Cr(CO)_6]$, $[Mo(CO)_6]$, $[W(CO)_6]$, $[Mn_2(CO)_{10}]$, $[Re_2(CO)_{10}]$, $[Fe_2(CO)_9]$, $[Ru_3(CO)_{12}]$, $[Os_3(CO)_{12}]$, $[Co_2(CO)_8]$, $[Rh_6(CO)_{16}]$, and $[Ir_6(CO)_{16}]$ were obtained from Strem and Aldrich, and $[BMIm][BF_4]$ from IoLiTec (H_2O content $\ll$100 ppm; Cl^- content $\ll$50 ppm). Cyclohexene (p.A., purity > 99.5 %) was obtained from Sigma–Aldrich and used without further purification. All synthesis experiments were done using Schlenk techniques under argon since the metal carbonyls are hygroscopic and air sensitive. The IL was dried under high vacuum (10^{-3} mbar) for several days. TEM photographs were taken at room temperature from a carbon-coated copper grid on a Zeiss LEO 912 transmission electron microscope operating at an accelerating voltage of 120 kV.

Decomposition: Each decomposition reaction was carried out at least twice. Decomposition reactions to produce the M-NPs that were used in the catalysis in this work (M = Ru, Rh, Ir) were carried out five or more times.

Microwave: Decomposition by means of microwave irradiation was carried out under argon. In a typical reaction, the fine metal–carbonyl powder $[M_x(CO)_y]$ (M = Cr, Mo, W, Fe, Ru, Os, Co, Rh, Ir; 10.2 to 3.45 mg, respectively; see Table S2 in the Supporting Information) was dissolved/suspended ($\approx$1 h) under an argon atmosphere at room temperature in dried and deoxygenated $[BMIm][BF_4]$ (0.4 mL, 0.48 g) for a 0.5 wt % M/IL dispersion. For the synthesis of a 1 wt % M/IL dispersion the metal carbonyl $[M_x(CO)_y]$ (M = Ru, Rh, Ir; 37.9 to 25.9 mg) was suspended/dissolved ($\approx$1 h) under an argon atmosphere at room temperature in dried and deoxygenated $[BMIm][BF_4]$ (1.5 mL, 1.8 g). For the synthesis, the mixture was placed in a microwave (CEM, Discover) under an

inert argon atmosphere and the conversion was finished within 3 min at a power of 10 W.

Photolytic: Photolytic decompositions of a solution/dispersion of the metal carbonyl $[M_x(CO)_y]$ (19.4 to 55 mg, see Table S2 in the Supporting Information) in [BMIm][BF_4] (2.0 or 2.5 mL, 2.4 or 3.0 g, respectively) for a 0.5 wt% M/IL dispersion were carried out in a Kürner UV 1000 reactor (Kürner-Analysentechnik) in quartz tubes for 15 min under argon with a Hg UV lamp (1000 W, radiation range 200–400 nm).

Thermal: Thermal decompositions were carried out under argon in a vessel that was connected to an oil bubbler. In a typical experiment, the fine metal–carbonyl powder $[M_x(CO)_y]$ (M = Cr, Mo, W, Fe, Ru, Os, Co, Rh, Ir; 200 to 8 mg, respectively) was dissolved/suspended ($\approx$1 h) under argon at room temperature in [BMIm][BF_4] (2.5 mL, 3.0 g, density 1.208 g cm^{-3}) for a 0.2 to 1 wt% M/IL dispersion. The metal–carbonyl solution was slowly heated to 180–250 °C with a minimum of 10 °C above the $[M_x(CO)_y]$ decomposition temperature (see the Supporting Information). After cooling to room temperature under argon, an aliquot of the ILs was collected under an argon atmosphere for in situ TEM and DLS characterization.

Catalysis: Hydrogenation reactions were carried out in a 100 mL pressure reactor (HEL, AutoMATE) equipped with a gas-inducing impeller stirrer with online hydrogen-consumption monitoring. In a typical experiment, cyclohexene (20 mL, 0.2 mol) was added to the reactor with the Ru-, Rh-, or Ir-NP/[BMIm][BF_4] dispersion (1.5 mL (1.8 g) IL with 1 wt% Ru, Rh, or Ir; 18 mg (0.18 mmol) Ru or Rh, 18 mg (0.09 mmol) Ir). After purging with N_2, the mixture was heated to the desired temperature. After purging with H_2, the reactor was pressurized to the desired pressure (10 or 4 bar) and the stirring at 1400 rpm started. The progress of the reaction was monitored by the hydrogen consumption using a mass flow controller (Brooks). After having reached 95% conversion, adjudged by the H_2 consumption, the reactor was depressurized, the organic layer was decanted, and fresh cyclohexene (20 mL) was added. The cyclohexene-to-cyclohexane conversion was verified by GC (Hewlett Packard HP 6890 Series GC system) equipped with a DB-1 capillary column and FID detector.

Metal analyses were performed using a Perkin–Elmer Optima 4300 ICP-AES to check for the leaching of metal in the reaction filtrate. The reaction mixture was evaporated to remove the solvent and the residue was dissolved in concentrated nitric acid (10 mL).

Acknowledgements

We thank Dr. T. J. S. Schubert from IoLiTec (Ionic Liquids Technologies GmbH, Denzlingen, Germany) for the donation of ionic liquids, Prof. W. Bannwarth and Dr. L. Rumi for access to the microwave CEM system type Discover, and the DFG for financial support through grant Ja466/16-1 (for K.A.S., collaboration with Jordan) and through grant Ja466/17-1.

[1] P. Braunstein, J. Rosé in *Metal Clusters in Chemistry, Vol. 2* (Eds: P. Braunstein, L. A. Oro, P. R. Raithby), Wiley-VCH, Weinheim **2001**, Chapter 2, pp. 616–677.
[2] A. H. Lu, E. L. Salabas, F. Schüth, *Angew. Chem.* **2007**, *119*, 1242–1266; *Angew. Chem. Int. Ed.* **2007**, *46*, 1222–1244.
[3] A. Gedanken, *Ultrason. Sonochem.* **2004**, *11*, 47–55.
[4] C. N. R. Rao, S. R. C. Vivekchand, K. Biwas, A. Govindaraj, *Dalton Trans.* **2007**, 3728–3749.
[5] Y. Mastai, A. Gedanken in *Chemistry of Nanomaterials, Vol. 1* (Eds.: C. N. R. Rao, A. Müller, A. K. Cheetham), Wiley-VCH, Weinheim, **2004**, p. 113.
[6] D. Mahajan, E. T. Papish, K. Pandya, *Ultrason. Sonochem.* **2004**, *11*, 385–392.
[7] J. Park, J. Joo, S. G. Kwon, Y. Jang, T. Hyeon, *Angew. Chem.* **2007**, *119*, 4714–4745; *Angew. Chem. Int. Ed.* **2007**, *46*, 4630–4660.
[8] A. Taubert, Z. Li, *Dalton Trans.* **2007**, 723–727.
[9] E. Redel, R. Thomann, C. Janiak, *Inorg. Chem.* **2008**, *47*, 14–16.
[10] T. Gutel, J. Garcia-Antón, K. Pelzer, K. Philippot, C. C. Santini, Y. Chauvin, B. Chaudret, J.-M. Basset, *J. Mater. Chem.* **2007**, *17*, 3290–3292.
[11] L. S. Ott, R. G. Finke, *Inorg. Chem.* **2006**, *45*, 8382–8393.
[12] G. S. Fonseca, A. P. Umpierre, P. F. P. Fichtner, S. R. Teixeira, J. Dupont, *Chem. Eur. J.* **2003**, *9*, 3263–3269.
[13] Z. Li, A. Friedrich, A. Taubert, *J. Mater. Chem.* **2008**, *18*, 1008–1014.
[14] P. Migowski, G. Machado, L. M. Rossi, G. Machado, J. Morais, S. R. Teixeira, M. C. M. Alves, A. Traverse, J. Dupont, *Phys. Chem. Chem. Phys.* **2007**, *9*, 4814–4821.
[15] J. M. Zhu, Y. H. Shen, A. J. Xie, L. G. Qiu, Q. Zhang, X. Y. Zhang, *J. Phys. Chem. B* **2007**, *111*, 7629–7639.
[16] M. A. Firestone, M. L. Dietz, S. Seifert, S. Trasobares, D. J. Miller, N. J. Zaluzec, *Small* **2005**, *1*, 754–760.
[17] K. Peppler, M. Polleth, S. Meiss, M. Rohnke, J. Z. Janek, *Phys. Chem.* **2006**, *220*, 1507–1527.
[18] A. Safavi, N. Maleki, F. Tajabadi, E. Farjami, *Electrochem. Commun.* **2007**, *9*, 1963–1986.
[19] K. Kim, C. Lang, P. A. Kohl, *J. Electrochem. Soc.* **2005**, *152*, E9.
[20] G. Schmid in *Nanoparticles*, Wiley-VCH, Weinheim, **2004**, pp. 185–238.
[21] D. Astruc, F. Lu, J. R. Aranzaes, *Angew. Chem.* **2005**, *117*, 8062–8083; *Angew. Chem. Int. Ed.* **2005**, *44*, 7852–7872.
[22] M. Antonietti, D. Kuang, B. Smarly, Y. Zhou, *Angew. Chem.* **2004**, *116*, 5096–5100; *Angew. Chem. Int. Ed.* **2004**, *43*, 4988–4992.
[23] J. Krämer, E. Redel, R. Thomann, C. Janiak, *Organometallics* **2008**, *27*, 1976–1978.
[24] E. Redel, J. Krämer, R. Thomann, C. Janiak, *J. Organomet. Chem.* **2009**, *694*, 1069–1075.
[25] E. Redel, R. Thomann, C. Janiak, *Chem. Commun.* **2008**, 1789–1791.
[26] E. Redel, J. Krämer, R. Thomann, C. Janiak, *GIT Labor-Fachzeitschrift* **2008**, 400–404.
[27] D. Bogdal in *Microwave-Assisted Organic Synthesis*, Elsevier, New York, **2006**. pp. 47–189.
[28] A. L. Buchachenko, E. L. Frankevich in *Chemical Generation and Reception of Radio- and Microwaves*, Wiley-VCH, Weinheim, **1993**, pp. 41–56; V. K. Ahluwulia in *Alternative Energy Processes in Chemical Synthesis*, Alphas Science International, Oxford (UK), **2008**.
[29] J. Berlan, P. Giboreau, S. Lefeuvre, C. Marchand, *Tedrahedron Lett.* **1991**, *32*, 2363–2366.
[30] F. Langa, P. De La Cruz, A. De La Hoz, A. Diez-Barra, *Contemp. Org. Synth.* **1997**, *4*, 373–386.
[31] L. Perreux, A. Loupy, *Tetrahedron* **2001**, *57*, 9199–9223.
[32] A. Stadler, C. O. Kappe, *J. Chem. Soc. Perkin Trans. 2* **2000**, 1363–1368.
[33] A. Stadler, C. O. Kappe, *Eur. J. Org. Chem.* **2001**, 919–925.
[34] P. Wasserscheid, W. Keim, *Angew. Chem.* **2000**, *112*, 3926–3945; *Angew. Chem. Int. Ed.* **2000**, *39*, 3772–3789.
[35] J. Dupont, *J. Brazil Chem. Soc.* **2004**, *15*, 341–350; C. S. Consorti, P. A. Z. Suarez, R. F. de Souza, R. A. Burrow, D. H. Farrar, A. J. Lough, W. Loh, L. H. M. da Silva, J. Dupont, *J. Phys. Chem. B* **2005**, *109*, 4341–4349; J. Dupont, P. A. Z. Suarez, R. F. de Souza, R. A. Burrow, J.-P. Kintzinger, *Chem. Eur. J.* **2000**, *6*, 2377–2381.
[36] E. J. W. Verwey, J. T. G. Overbeek in *Theory of the Stability of Lyophobic Colloids*, Dover Publications Mineola, New York, **1999**, pp. 1–218.
[37] A. N. Shipway, E. Katz, I. Willner, *ChemPhysChem* **2000**, *1*, 18–25.
[38] T. Cassagneau, J. H. Fendler, *J. Phys. Chem. B* **1999**, *103*, 1789–1793.
[39] C. D. Keating, K. K. Kovaleski, M. J. Natan, *J. Phys. Chem. B* **1998**, *102*, 9404–9413.
[40] A. P. Umpierre, G. Machado, G. H. Fechner, J. Morais, J. Dupont, *Adv. Synth. Catal.* **2005**, *347*, 1404–1412.
[41] L. S. Ott, R. G. Finke, *Coord. Chem. Rev.* **2007**, *251*, 1075–1100.

[42] B. L. Bhargava, S. Balasubramanian, M. L. Klein, *Chem. Commun.* **2008**, 3339–3351.
[43] T. J. Gannon,, G. Law, R. P. Watson, A. J. Carmichael, K. R. Seddon, *Langmuir* **1999**, *15*, 8429–8434.
[44] J. N. Canongio Lopes, M. F. C. Gomes, A. A. H. Padua, *J. Phys. Chem. B* **2006**, *110*, 16816–16818.
[45] J. N. Canongia Lopes, A. A. H. Padua, *J. Phys. Chem. B* **2006**, *110*, 3330–3335.
[46] G. Law, R. P. Watson, A. J. Carmichael, K. R. Seddon, *Phys. Chem. Chem. Phys.* **2001**, *3*, 2879–2885.
[47] R. A. Sheldon, *Chem. Commun.* **2008**, 3352–3365.
[48] P. Wasserscheid, T. Welton in *Ionic Liquid in Synthesis, Vol. 1*, Wiley-VCH, Weinheim, **2007**, pp. 325–350.
[49] V. Parvulescu, C. Hardacre, *Chem. Rev.* **2007**, *107*, 2615–2665.
[50] D. Astruc, *Nanoparticles and Catalysis*, Wiley-VCH, Weinheim, **2007**.
[51] H.-G. Elias in *Makromoleküle, Vol. 3*, Wiley-VCH, Weinheim. **2001**, pp. 368–454.
[52] B. K. Hodnett in *Heterogeneous Catalytic Oxidations*, Wiley-VCH, Weinheim. **2000**, pp. 240–263.
[53] J. Dupont, G. S. Fonseca, A. P. Umpierre, P. F. P. Fichtner, S. R. Texeira, *J. Am. Chem. Soc.* **2002**, *124*, 4228–4229.
[54] L. M. Rossi, G. Machado, P. F. P. Fichtner, S. R. Teixeira, J. Dupont, *Catal. Lett.* **2004**, *92*, 149–155.
[55] J. Huang, T. Jiang, B. Han, H. Gao, Y. Chang, G. Zhao, W. Wu, *Chem. Commun.* **2003**, 1654–1655.
[56] E. T. Silveira, A. P. Umpierre, L. M. Rossi, G. Machado, J. Morais, G. V. Soares, I. L. R. Baumvol, S. R. Teixeira, P. F. P Fichtner, J. Dupont, *Chem. Eur. J.* **2004**, *10*, 3734–3740.
[57] STOE WinXPow version 1.10, data base, STOE & Cie GmbH, Germany, **2002**.
[58] J. M. Praetorius, C. M. Crudden, *Dalton Trans.* **2008**, 4079–4094.
[59] G. Ertl, H. Knözinger, J. Weitkamp in *Handbook of Heterogenous Catalysis, Vol. 9*, Wiley-VCH, Weinheim, **2008**.
[60] J. D. Scholten, G. Ebeling, J. Dupont, *Dalton Trans.* **2007**, 5554–5560.
[61] L. Durán Pachón, G. Rothenberg, *Appl. Organomet. Chem.* **2008**, *22*, 288–299.
[62] Y. Lin, R. G. Finke, *Inorg. Chem.* **1994**, *33*, 4891–4910.
[63] B. J. Hornstein, J. D. Aikon III, R. G. Finke, *Inorg. Chem.* **2002**, *41*, 1625–1638.
[64] J. A. Widegren, M. A. Bennett, R. G. Finke, *J. Am. Chem. Soc.* **2002**, *124*, 10301–10310.
[65] L. Gonzalez-Tejuca, K. Aika, S. Namba, J. Turkevich, *J. Phys. Chem.* **1977**, *81*, 1399–1406.
[66] H. G. Manyar, D. Weber, H. Daly, J. M. Thompson, D. W. Rooney, L. F. Gladden, E. H. Stitt, J. J. Delgado, S. Bernal, C. Hardacre, *J. Catal.* **2009**, *265*, 80–88.
[67] C. Hardacre, E. A. Mullan, D. W. Rooney, J. M. Thompson, *J. Catal.* **2005**, *232*, 355–365; C. Hardacre, E. A. Mullan, D. W. Rooney, J. M. Thompson, G. S. Yablonsky, *Chem. Eng. Sci.* **2006**, *61*, 6995–7006.

Received: November 24, 2009

Please note: Minor changes have been made to this publication in *Chemistry–A European Journal* Early View. The Editor.

Published online: February 24, 2010

